Available online at www.sciencedirect.com
SCIENCE DIRECT
Journal of Photochemistry and Photobiology A: Chemistry 181 (2006) 246–256
Journal of Photochemistry and Photobiology A:Chemistry
www.elsevier.com/locate/jphotochem

Secondary amino group as charge donor for the excited state intramolecular charge transfer reaction in *trans*-3-(4-monomethylamino-phenyl)-acrylic acid: Spectroscopic measurement and theoretical calculations

Amrita Chakraborty, Samiran Kar [1], Nikhil Guchhait *

Department of Chemistry, University of Calcutta 92, A.P.C. Road, Kolkata 700009, India

Received 16 August 2005; received in revised form 25 October 2005; accepted 1 December 2005
Available online 2 February 2006

Abstract

The emission properties of a synthesized donor–acceptor substituted aromatic system *trans*-3-(4-monomethylamino-phenyl)-acrylic acid (*t*-MMPAA) have been investigated both experimentally and theoretically. The molecule *t*-MMPAA shows dual fluorescence in polar solvents. The normal emission band is assigned to be arising from the locally excited state whereas the anomalous, solvent dependent, red shifted emission band arises from a twisted transient emissive state. Solvent dependency of the large Stokes shifted emission band and high dipole moment of the excited state support charge transfer character of the twisted excited state. Potential energy curves along the two possible twisting coordinates have been calculated for the ground and excited states both in vacuo and in polar aprotic acetonitrile solvent using time dependent density functional theory (TDDFT) and time dependent density functional theory including polarized continuum model (TDDFT-PCM), respectively. Both the twisted paths, i.e., along the donor (–NHMe) and acceptor (–CH=CHCOOH) groups, favor the formation of stable twisted excited state, but the twisting through acceptor path is energetically favorable (low barrier height) than the donor path. However, localized nitrogen lone pair supports TICT process by twisting along the donor path. A more stabilized calculated twisted state in acetonitrile solvent correlates well with the solvent dependent red shifted emission.

Keywords: *trans*-3-(4-Monomethylamino-phenyl)-acrylic acid; Dual fluorescence; TICT; TDDFT

1. Introduction

Since the first report on dual fluorescence of *p*-(*N*,*N*-dimethylamino)-benzonitrile (DMABN) by Lippert and Luder [1], intramolecular charge transfer processes are the attractive field of research due to various applications in the basic and applied fields. Numerous compounds having donor–acceptor moiety with subunits connected by a single bond [2,3] emitting dual fluorescence are known by now, but the origin of this unusual property is still not completely understood, and various mechanisms have been suggested since then. To explain the dual fluorescence of these types of compounds in polar solvents, Grabowski and co-workers [4] proposed a scheme involving intramolecular charge transfer with a 90° twisting motion of the donor group, leading to the formation of an emissive transient species called twisted intramolecular charge transfer state (TICT). Grabowski et al. [5] also had shown that twisting of the acceptor moiety causes no L_a emission from the perpendicular conformer. Alternative models like planar intramolecular charge transfer (PICT) [6], wagging intramolecular charge transfer (WICT) and rehybridization intramolecular charge transfer (RICT) [7,8] have been proposed to explain the dual fluorescence phenomenon in different donor–acceptor systems. Recent experimental and computational studies are, however, in large number in favor of TICT model [9–15].

In this work, we have investigated dual fluorescence of *t*-MMPAA in different solvents and applied density functional theory (DFT) to understand qualitatively the mechanism of photoinduced ICT reaction. Most of the molecules so far investigated for these studies mainly have tertiary amino such as *N*,*N*-dimethylamino group as charge donor. So far our knowledge goes to there are only two examples where secondary amino

* Corresponding author. Tel.: +91 033 2350 8386
E-mail addresses: nguchhait@yahoo.com, nikhil.guchhait@rediffmail.com (N. Guchhait).
[1] Present address: CHEMGEN Pharma International, Dr. Siemens Street, Block GP, Sector V, Salt Lake City, Kolkata 700 091, India.

1010-6030/$ – see front matter © 2006 Elsevier B.V. All rights reserved.
doi:10.1016/j.jphotochem.2005.12.004

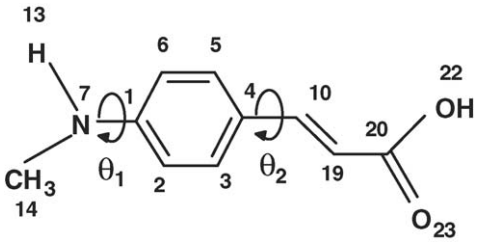

Scheme 1. *trans*-3-(4-Monomethylamino-phenyl)-acrylic acid (*t*-MMPAA), θ_1 and θ_2 are torsional angles at the donor and acceptor sides.

groups with ortho substituted methyl group are used as a charge donor for the excited state ICT reaction [7,16]. It is proposed that the ortho substitution forced the secondary amino group to be in the out of plane of the benzene ring and hence, TICT emission is observed. We have synthesized a system with secondary amino group without ortho substitute as charge donor, namely *trans*-3-(4-monomethylamino-phenyl)-acrylic acid (Scheme 1) and investigated excited state ICT reaction spectroscopically. The presence of unsaturated double bond at the acceptor side provides extra flexibility to the molecule. We have studied the photophysical properties of *t*-MMPAA by absorption and emission spectroscopy. Dual fluorescence phenomenon has been studied by exploring potential energy surfaces of the excited states along the two possible twist coordinates, i.e., (i) twisting of donor (–NHMe) [9] and (ii) acceptor group (–CH=CHCOOH) [17,18], using TDDFT method with inclusion of solvent effect using polarized continuum model (PCM) [19].

2. Experimental details

2.1. Materials

p-Nitro benzaldehyde and ethyl (triphenyl phosphanylidene) acetate (Ph_3P=CH-COOEt) in dry dichloromethane were stirred at room temperature for 24 h. Generated nitro product was reduced by using zinc and saturated aqueous ammonium chloride solution in methanol at 50 °C to produce ethyl-3-(4-aminophenyl)-acrylate. Then one hydrogen atom of amino group was blocked by di-*tert* butyl pyrocarbonate (BOC-anhydride) in presence of triethylamine in THF to produce ethyl-3(4-[*N*-(*tert*-butoxycarbonyl)-amino]-phenyl)-acrylate. In the next step, hydrogen atom of BOC protected amino group was replaced by methyl group using methyl iodide in presence of sodium hydride base in DMF solvent at 0 °C. Then BOC group was removed by using trifluroaccetic acid in dichloromethane to produce ethyl-3(4-methylamino-phenyl)-acrylate. The product was hydrolyzed by using lithium hydroxide in THF and water mixture to get the desire product *trans*-3-(4-methylamino-phenyl)-acrylic acid [20]. The product was purified through silica gel column chromatography and finally recrystalized to get pure compound. ^{1}H NMR (300 MHz, $CDCl_3$) δ 2.88 (s, 3H), 6.18 (d, J = 15.81 Hz, 1H), 6.56 (d, J = 8.61 Hz, 2H), 7.39 (d, J = 8.58 Hz, 2H), 7.67 (d, J = 15.81 Hz, 1H). FTIR (ν cm^{-1}) 509, 553, 819, 1176, 1259, 1313, 1431, 1529, 1596, 1656, 2819, 2900, 2929, 3371, 3408.

Spectroscopic grade solvents methanol, isopropanol, chloroform, hexane, acetonitrile from Spectrochem-UV and ethanol from E. Merck were used after vacuum distillation. All solvents were checked for any fluorescence in the desired wavelength before emission studies. Sulphuric acid from E. Merck was used as supplied. Triple distilled water was used for making all aqueous solutions.

2.2. Steady state and time resolved spectral measurements

The absorption and emission spectra of *t*-MMPAA were recorded on a Hitachi UV/VIS U-3501 spectrophotometer and Perkin Elmer LS50B fluorimeter, respectively. All the spectral measurements were done at $\sim 10^{-6}$ M concentration of solute in order to avoid aggregation and self-quenching.

Time Master Fluorimeter from Photon Technology International (PTI) was used to measure fluorescence lifetime [21]. The sample was excited at 315 nm using a thyratron gated nitrogen flash lamp (width ~1.5 ns). The system measures fluorescence lifetime at a flash rate of 25 kHz using PTI's patented strobe technique and gated detection method. Lamp profiles were measured at the excitation wavelength using Ludox as the scatterer using slits with a band pass of 3 nm. Intensity decay curves were fitted as a sum of exponential terms: $F(t) = \sum_i \alpha_i \exp(-t/\tau_i)$ where α_i is a pre-exponential factor representing the fractional contribution to the time resolved decay of the component with a life time τ_i. The Software FeliX32 is used for data acquisition and analysis. The decay parameters were recovered using a non-linear least squares iterative fitting procedure based on Marguardt algorithms [22]. The quality of fit has been assessed over the entire decay, including the rising edge, and tested with a plot of weighted residuals and the other statistical parameters, e.g., the reduced χ^2 and the Durbin–Watson parameters ($1.6 < DW > 2.0$) [23].

2.3. Computational details

All structural and potential energy surface calculations were performed using Gaussian 03 Package [24]. Ground state geometry have been optimized with B3LYP hybrid functional and 6-31++g(d,p) basis set. Excitation energies were calculated using time dependent density functional theory (TDDFT) implemented in the Gaussian using the same functional and basis set. Computed excitation energies are the vertical transition energy without zero point correction. We also extended our calculations in solvated system using non-equilibrium TDDFT-PCM model. Calculations on potential energy surface (PES) were pursued along the twist coordinate separately at the donor and acceptor sites. We have used rotational angle θ_1 and θ_2 (shown in Scheme 1) to get the twisting of donor (–NHMe) and acceptor (–CH=CHCOOH) group, respectively. One limitation is that the above-calculated PES only corresponds to the cut off PE-hyper surface along the twisting angle as no geometry optimization of the various excited states has been performed. This approach, i.e., the use of ground state optimized geometry as a basis for the representation of the excited state structure, has

been successfully applied in many recent scientific publications [10–12,25–27]. However, some groups have performed relaxed calculations to get the excited state PESs [28–30]. Radiative lifetime (τ) have been computed for the spontaneous emission using the following equation [31],

$$\tau(\mathrm{s}) = \frac{3}{2f\nu^2}$$

where 'ν' and 'f' are the calculated transition energy in cm^{-1} and oscillator strength, respectively.

3. Results and discussion

3.1. Absorption spectra

The absorption spectra of *trans*-3-(4-monomethylaminophenyl)-acrylic acid ($\sim 10^{-6}$ M) in non-polar, polar and hydrogen bonding solvents are shown in Fig. 1. As seen in the spectra, the molecule *t*-MMPAA shows absorption bands at ~315 and ~350 nm. These two bands are assigned to the transition from ground (S_0) to S_2 (L_b) and S_1 (L_a) states (Platt's notation), respectively [32]. It is found that the position of the higher energy absorption peak is independent on solvent polarity whereas the lower energy absorption band shows its dependency on both the polarity and hydrogen bonding ability of the solvent. In protic solvent, the lower energy absorption band shifts towards the blue region and it seems that two bands almost merged in water and methanol solvent. The lower energy absorption band shows slight red shift depending on the polarity of the aprotic solvent. The hypsochomic shift of lower energy absorption band in protic solvent indicates higher stability of the system in the ground state due to possible intermolecular hydrogen bonding between solute and solvent (Scheme 2).

3.2. Emission spectra

The emission spectra of *t*-MMPAA in different solvents are shown in Fig. 2a and the observed band maxima are presented in Table 1. In non-polar solvent such as hexane and heptane, upon 335 nm excitation, *t*-MMPAA shows a single fluorescence band at ~390 nm which is ascribed to the emission from the locally excited state (LE). But for the same excitation dual fluorescence is observed in polar solvents. Apart from the weak higher energy LE emission band (~390 nm), a solvent's polarity dependent emission band is observed at ~440 nm. Comparing with other studied systems we have assigned the lower energy emission band to the emission from the charge transfer (CT) state

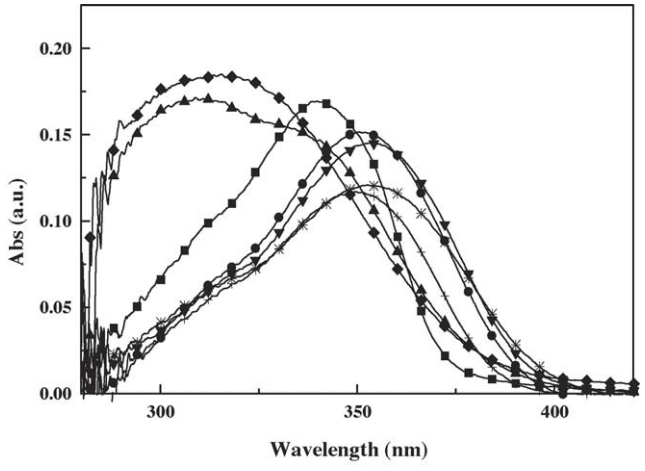

Fig. 1. Absorption spectra of *t*-MMPAA at room temperature in (-●-) ACN, (-♦-) water, (-▲-) MeOH, (-*-) EtOH, (-+-) THF, (-▼-) chloroform, (-■-) and hexane solvents.

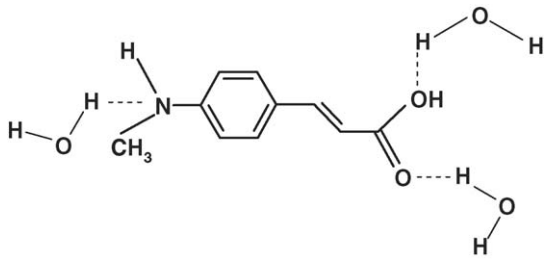

Scheme 2. Possible hydrated cluster.

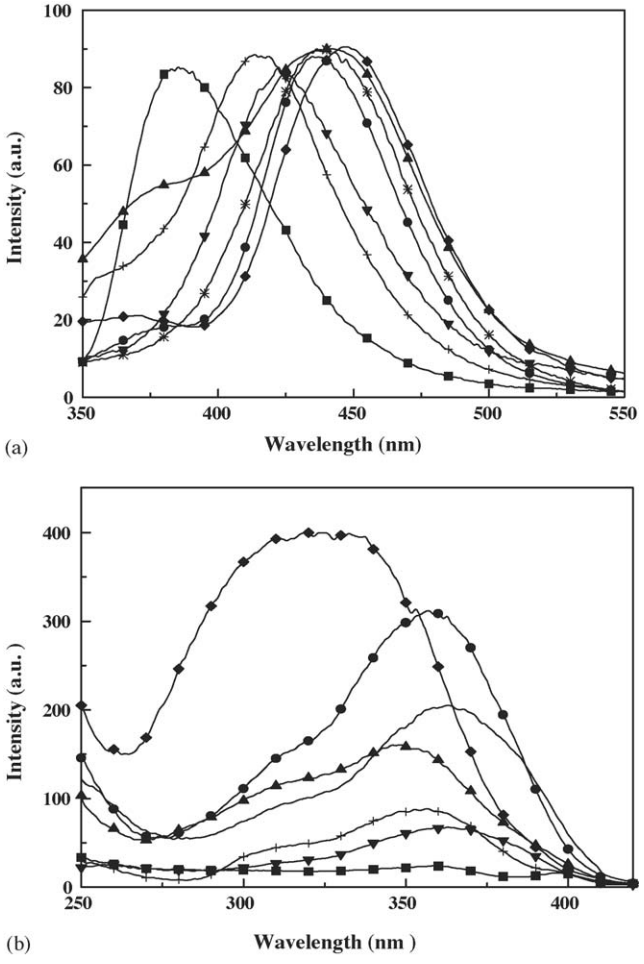

Fig. 2. (a) Emission spectra (λ_{ext} = 335 nm) of *t*-MMPAA at room temperature in (-●-) ACN, (-♦-) water, (-▲-) MeOH, (-*-) EtOH, (-+-) THF, (-▼-) chloroform and (-■-) hexane solvents. (b) Excitation spectra of *t*-MMAA at room temperature in (-●-) ACN, (-♦-) water, (-▲-) MeOH, (-*-) EtOH, (-+-) THF, (-▼-) chloroform and (-■-) hexane solvents (emission was monitored at the strong fluorescence band, see Table 1).

Table 1
Spectroscopic parameters obtained from absorption and emission band maxima of *t*-MMPAA in different solvents

Solvent	λ_{abs} (nm)	λ_{flu} (nm)	ν_{abs} (cm^{-1})	ν_{flu} (cm^{-1})	$\Delta\nu$ (cm^{-1})
Hexane	339, 315	385	29411	25974	3524
Dioxane	348, 315	411	28735	24330	4405
Chloroform ($CHCl_3$)	354, 318	423	28248	23640	4608
Tetrahydrof uran (THF)	347, 315	382, 417	28818	23981	4837
Acetonitrile (ACN)	352, 315	380, 437	28409	22883	5526
Ethanol (EtOH)	354, 315	380, 439	28248	22779	5469
Methanol (MeOH)	331, 315	382, 442	30211	22624	7587
Water	315 (broad)	371, 448	31746	22321	9425

[33]. It is found that the peak positions of the emission bands are independent on excitation wavelength over a large range of the absorption band. The excitation spectra (Fig. 2b) of both the bands are independent of emission wavelength and agree reasonably well with the absorption spectrum. So we can say that only one species is present in the ground state and CT band is generated through the LE state. Emission in binary solvent mixture (methylcyclohexane + ethanol) is shown in Fig. 3. As seen in Fig. 3, with increasing the solvent polarity by adding ethanol to methylcyclohexane solution the intensity of the CT band (~440 nm) increases with concomitant decrease in the intensity of the LE state emission (~390 nm band). This indicates also that the CT state is generated from the LE state [33]. Cazeau-Dubroca et al. proposed that tetragonal arrangement of amine side due to formation of hydrogen bond with protic solvent in the ground state favors TICT process [34].

A qualitative analysis of the red shift of lower energy emission band indicates that the emissive species must possess high dipolar character. According to Lippert-Mataga relation the emission maxima of the charge transfer band of this type of donor–acceptor systems shows a linear dependency with the solvent parameter Δf and can be expressed by the following equations [35],

$$\nu_a - \nu_f = \left[\frac{2}{hca^3}\right]\Delta f[\mu^* - \mu]^2$$

$$\Delta f = \left[\frac{\varepsilon - 1}{2\varepsilon + 1}\right] - \left[\frac{n^2 - 1}{2n^2 + 1}\right]$$

where h, c, a, ε, n, μ^* and μ are Planck's constant, speed of light, radius of the cavity of the fluorophore, dielectric constant of the medium, refractive index, dipole moment of the excited and ground state, respectively, the absorption and emission frequencies are ν_a and ν_f, respectively. The plot of Stokes shift and solvent parameter (Δf) is shown in Fig. 4(a). A linear relationship between the Stokes shift and solvent parameter in aprotic solvents predicts large dipole moment of the emissive species. The calculated dipole moment by solvatochromic method for the CT and LE state are 12.98 and 9.08 D, respectively. The large change in dipole moment of the CT state (12.98 D) with respect

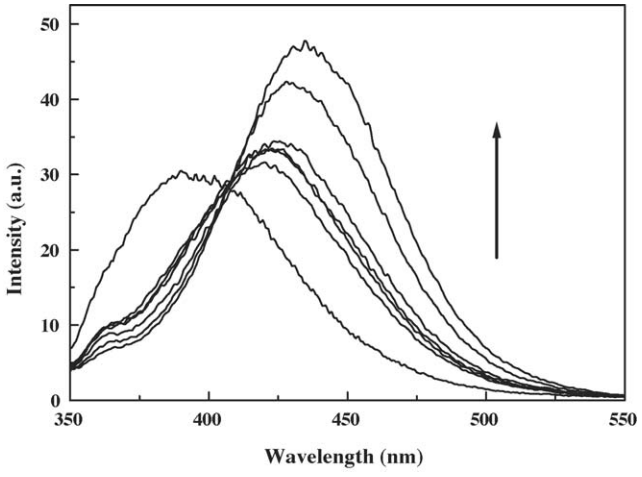

Fig. 3. Fluorescence emission spectra (λ_{ext} = 335 nm) of *t*-MMPAA in methylcyclohexane and ethanol mixture (arrow indicates increase in ethanol concentration).

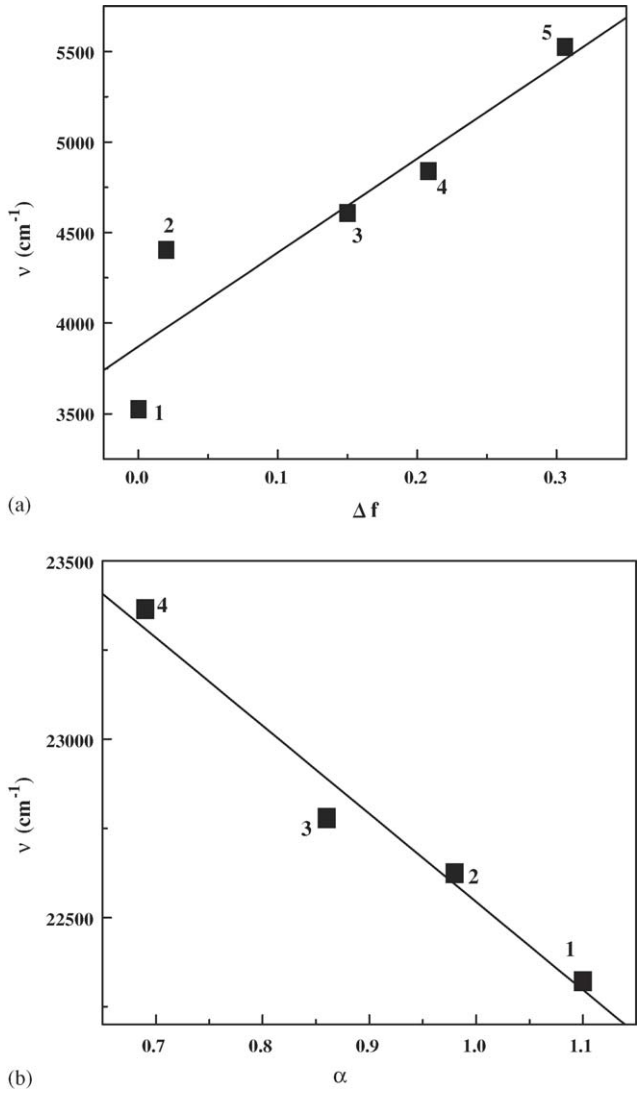

Fig. 4. Plot of (a) Stokes shift vs. solvent parameter (Lippert plot) of *t*-MMPAA (1) hexane, (2) dioxane, (3) $CHCl_3$, (4) THF, (5) ACN of *t*-MMPAA; (b) plot of hydrogen bonding parameter (α) vs. florescence band position of *t*-MMPAA in (1) water, (2) methanol, (3) ethanol and (4) isopropanol.

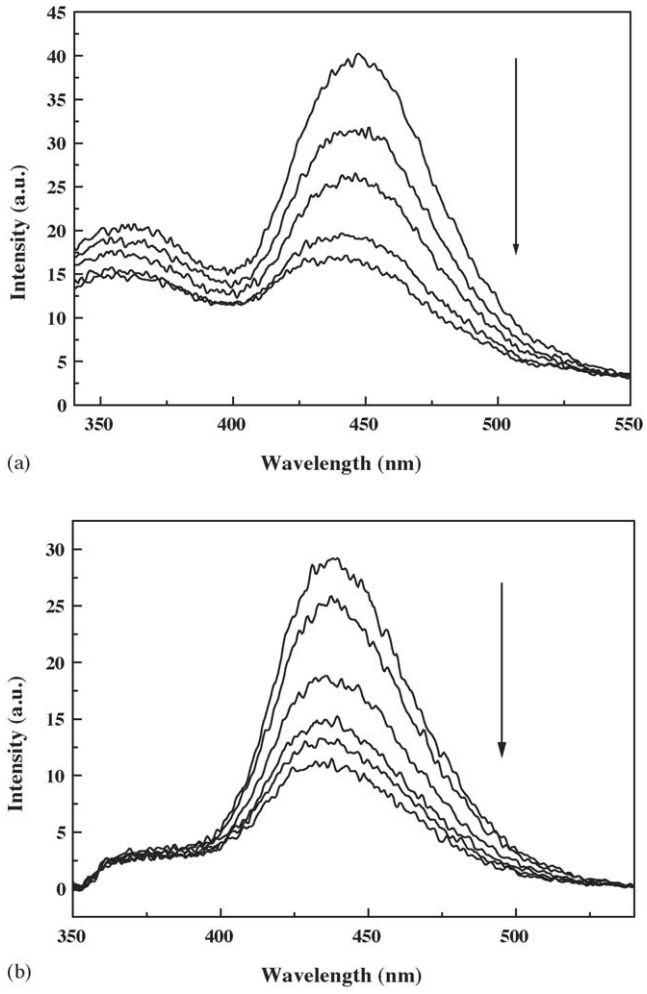

Fig. 5. Temperature dependent emission spectra (λ_{ext} = 335 nm) of *t*-MMPAA in (a) water and in (b) ACN solvent (arrow indicates increase of temperature from 273 to 313 K with 10 K increment).

to the ground state (6.75 D) supports the fact that full charge transfer occurs through the relaxation of LE state to CT state and hence, solvent dependent red shifted emission is observed [36].

A deviation from linearity of Stokes shift versus Δf in protic solvents reveals that there must be some additional factor, which is responsible for this non-linearity. Usually, protic solvents have a tendency to form intermolecular hydrogen bonded complex and the weak hydrogen bonding interaction significantly influences the properties in the ground and excited states. As seen in Fig. 4(b), a linear dependency is found between the fluorescence maxima of the red shifted band and the hydrogen bonding parameter (α) in protic solvents [37]. This observation points out that intermolecular hydrogen bonding has some effect in the excited state ICT process [38]. To confirm the presence of hydrogen bonding we have measured temperature dependent emission spectra both in water and acetonitrile solvents. As seen in Fig. 5, it is found that the intensity of CT emission band decreases with increasing temperature in water and acetonitrile solvent. In acetonitrile the intensity of LE emission band is almost intact whereas the same LE emission in water decreases with increasing temperature. The decrease of intensity of CT emission could be due to the increase of non-radiative decay with increase of temperature. But the decrease in intensity of the LE emission indicates the breaking of intermolecular hydrogen bonding of the solvated complex.

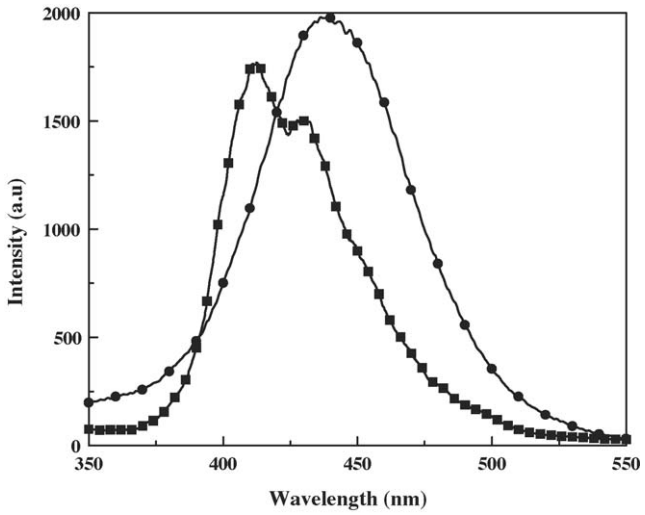

Fig. 6. Emission spectra of *t*-MMPAA in (-●-) ethanol at room temperature and (-■-) ethanol glass matrix at 77 K.

The most notable observations are the fluorescence spectra of *t*-MMPAA in 77 K. As seen in Fig. 6, the fluorescence spectrum of *t*-MMPAA at 77 K in ethanol glass matrix shows a blue shift with respect to its room temperature spectra. This blue shift may reflect the change in solvent properties such as polarity, polarizibility and viscosity upon decreasing of temperature. The high viscosity of the 77 K glass matrix also inhibits the relaxation process from LE to CT state through the twisting path. As twisting motion is hindered only emission from LE state is observed in low temperature glass matrix. From this observation we can say that the twisting motion may be responsible for the excited state dual emission process.

The absorption and emission spectra of *t*-MMPAA molecule in presence of acid provide an interesting observation. Fig. 7a depicts the effect of acid on the absorption spectra of *t*-MMPAA in water. Addition of 2N sulphuric acid causes a drastic change in the absorption spectra. A new band appears at ~297 nm with the expense of ~315 nm band. The H^+ ion of acid can bind to the lone pair of nitrogen and the molecule may behave like a benzene type of chromophore connected to a conjugated double bond. Thus, the π–π* transition of benzene moiety connected to conjugated double bond shows a new absorption band at ~297 nm. The effect of acid on the emission spectra of *t*-MMPAA molecule is shown in Fig. 7b. Here also a new emission band arises at 380 nm at the expense of ~450 nm band. This emission basically arises from the protonated emissive species (Scheme 3). H^+ ion prefers to bind to the lone pair of nitrogen and hence, charge transfer process is absent in the excited state. These observations also suggests that CT band is a n–π* type of transition. Effect of base on *t*-MMPAA shows only abstraction of H^+ from the acid group (–COOH) without shifting of band position.

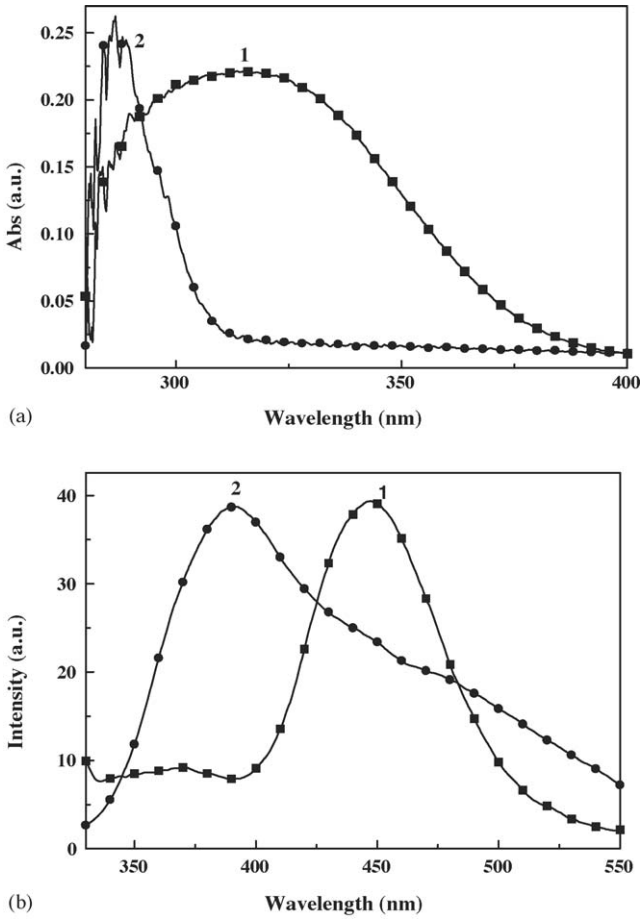

Fig. 7. (a) Absorption and (b) emission spectra (λ_{ext} = 290 nm) of *t*-MMPAA in (1) water, (2) water + 2N sulphuric acid.

Table 2
Fluorescence lifetime data of *t*-MMPAA in different solvents

Solvent	λ_{ex} (nm)	λ_{em} (nm)	τ (ns)	χ^2	τ_{cal} (ns)
Hexane	315	380	3.75 ± 0.1	1.78	2.3
ACN	315	380	3.29 ± 0.2	0.95	2.3
		430	0.36 ± 0.03	1.089	
Water	315	380	2.56 ± 0.2 (12%)	0.92	–
			0.66 ± 0.04 (88%)		

3.3. Lifetime measurements

The fluorescence lifetime values and the decay curves of *t*-MMPAA in different solvents are presented in Table 2 and Fig. 8, respectively. In hexane, the 380 nm emission is strictly monoexponential with decay time 3.75 ns and it is 3.29 ns in ACN solvent. In ACN the fluorescence at 430 nm is also monoexponential with decay time 0.36 ns. Charge transfer emission band has a shorter lifetime than the normal emission (LE) [39,40]. In water, on excitation at 315 nm and monitoring at 380 nm band, the emission decay is biexponential with lifetime 2.56 and 0.66 ns. The fast lifetime may be arising from the LE state of the hydrogen-bonded complex and the slow lifetime corresponds to emission from the unsolvated molecule. Weakly hydrogen bonding interaction highly effective in non-radiative transition and hence, the emission lifetime of the LE state reduces in protic solvent [41].

Table 3
Optimized geometry for the ground state of *t*-MMPAA in vacuo using DFT (B3LYP/6-31++g(d,p)) method

Bond	Calculated values (Å)	Angle/dihedral	Calculated values (°)
$R_{C1–C6}$	1.41	∠C14–N7–H13	117.0
$R_{C6–C5}$	1.38	∠N7–C1–C6	122.0
$R_{C5–C4}$	1.41	∠C10–C4–C5	123.9
$R_{C1–N7}$	1.37	∠C19–C10–C4	127.7
$R_{N7–C14}$	1.45	∠C20–C19–C10	123.9
$R_{N7–H13}$	1.0	∠O23–C20–C19	121.1
$R_{C4–C10}$	1.45	∠C14–N7–C1–C2	−11.8
$R_{C10–C19}$	1.35	∠C5–C4–C10–C19	0.0
$R_{C19–C20}$	1.46		
$R_{C20–O23}$	1.22		
$R_{C20–O22}$	1.36		

3.4. Quantum chemical calculation

We have tried to interpret the observed dual fluorescence phenomenon in the light theoretical calculation using TDDFT method. Ground state optimization have been done for all possible low energy structures using B3LYP hybrid functional and 6-31++g(d,p) basis set. It is noted that the optimized geometry of *t*-MMPAA yields a non-planar geometry with slightly pyramidal monomethylamino nitrogen (∠C14–N7–C1–C2 = −11.8). Some important optimized geometrical parameters for the ground state of *t*-MMPAA in vacuo are presented in Table 3. The calculated dipole moment for the ground state of global minimum structure is 6.75 D with the same basis set and functional, indicating unsymmetrical charge distribution in the ground state.

Experimental absorption band position, calculated absorption energies and oscillator strength values are presented in Table 4. Experimentally, the low energy absorption band in hexane solvent is observed at 339 nm (3.65 eV). The calculated transition energy in vacuo is 3.7 eV (335 nm) (We may consider that calculation in vacuo is almost equivalent to a non-polar solvent.) In acetonitrile solvent the experimental absorption band appears at 352 nm (3.52 eV). Calculation using TDDFT-non-

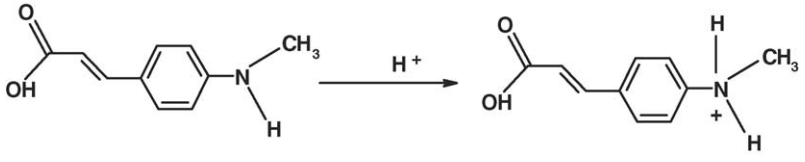

Scheme 3. Protonation reaction.

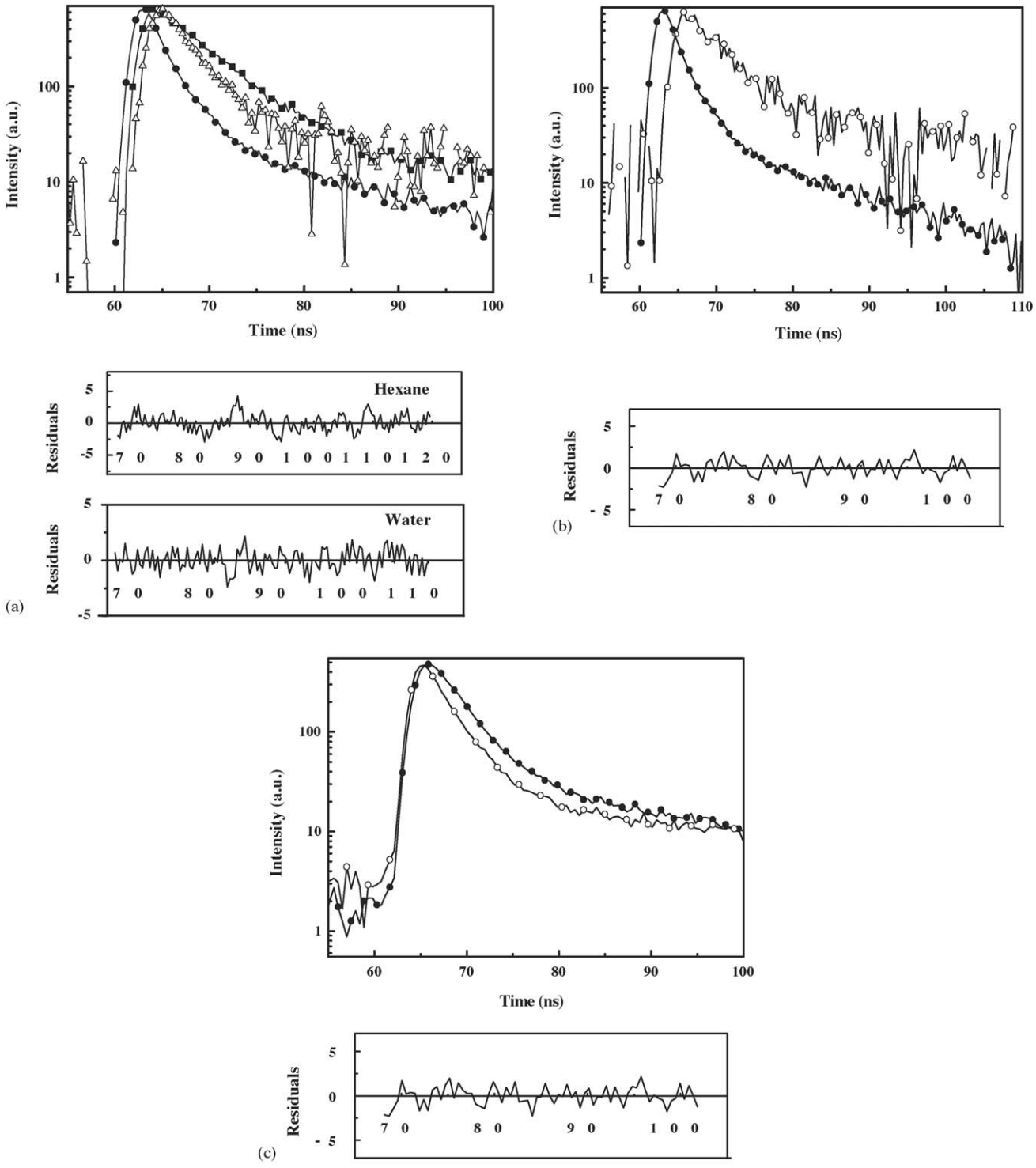

Fig. 8. Fluorescence decay curves of *t*-MMPAA in (a) (-△-) water (λ_{ext} = 315 nm, λ_{em} = 380 nm), (-■-) in hexane (λ_{ext} = 315 nm, λ_{em} = 380 nm), (-●-) lamp profile, (b) (-◯-) in ACN (λ_{ext} = 315 nm, λ_{em} = 380 nm), (-●-) lamp profile, (c) (-◯-) in ACN (λ_{ext} = 3\5 nm, λ_{em} = 430 nm), (-●-) lamp profile. Residuals are given at the bottom of each graph.

equilibrium PCM model in acetonitrile solvent shows transition energy value of 3.38 eV (365 nm). The deviation between the calculated and experimental transition energy is only 0.14 eV. The calculated vertical transition energy yields a good agreement with the experimental results. The computed transition energy in acetonitrile solvent shows a redshift (∼0.32 eV) relative to gas phase, and it is reasonable as acetonitrile is highly polar in nature. Red shifts of vertical transition energies in polar solvent both experimentally and theoretically indicate that the molecule is polar in nature. Presence of two absorption bands in polar and nonpolar solvents correlate well with the calculated energy of the first and second excited singlet states. As seen in Table 3,

Table 4
Computed parameters of *t*-MMPAA in vacuum and acetonitrile solvents using DFT method with B3LYP hybride functional and 6-31++g(d,p) basis set

	Absorption			Emission (twisting of the donor (–NHMe) group)			Emission (twist of the acceptor (–CH=CH COOH) group)		
	State	ΔE[a]	f[b]	State	ΔE[a]	f[b]	State	ΔE[a]	f[b]
Vacuo	S_1	3.7	0.724	S_1	3.16	0.0014	S_1	3.16	0.0002
	S_2	4.31	0.046	S_2	4.22	0.765	S_2	4.32	0.004
Acetonitrile	S_1	3.38	0.869	S_1	2.91	0.0015	S_1	2.89	0.0002
	S_2	4.28	0.046	S_2	4.01	0.7649	S_2	4.32	0.059

[a] ΔE = energy of S_n − energy of S_0 in eV.
[b] Oscillator strength (*f*).

the energy difference between the first and second excited state is not large. Theoretically the first excited state becomes more stabilized than the second excited state in polar solvent, so the energy difference between two states increases only in polar solvent.

The computed radiative lifetime [31] for the normal emission band is 2.3 ns both in hexane and acetonitrile solvent and the corresponding experimental values are 3.75 and 3.29 ns in hexane and acetonitrile, respectively (Table 2). The calculated radiative lifetime shows a good correlation with the experimental values.

Potential energy surfaces along the twist coordinate (θ_1) at the donor side both in vacuo and in acetonitrile are shown in Fig. 9. From the picture it is clear that the energy of the S_0 and S_2 states increases with twisting coordinate θ_1. On the other hand, the energy of S_1 state reaches a minimum at $\theta_1 = 78.0^\circ$. Herbich and Kapturkiewicz, in their through study of a long series of *p*-(9-anthryl)-*N*,*N*-dimethylaniline, found that the molecules relax to a state deviating from 90° conformation [42]. The nature of the first excited state along the twisting path reaches a full charge transfer character nearly at perpendicular ($\theta_1 = 78.0^\circ$) structure, as it is reflected by the value of oscillator strength and MO structure (Fig. 9a, inset and Fig. 10). As seen in the TDDFT wave functions in Fig. 10(a), first single excitation for the non-twisting geometry is π–π* (HOMO → LUMO) type where the contribution of lone pair orbital is made through the delocalized feature of HOMO. High oscillator strength ($f = 0.724$) value also supports this fact. At the twisted geometry ($\theta_1 = 78.0^\circ$), the CT state is also characterized by a singly excitation from HOMO (n) to LUMO (π*) (Fig. 10b). In this twist configuration the HOMO is now completely a lone pair orbital localized at the nitrogen atom of monomethylamino group. Low oscillator strength value ($f = 0.0014$) indicates the forbidden character of HOMO → LUMO transition, i.e., n → π* type of transition. Thus, localization of nitrogen lone pair in the twisted conformer favors charge transfer in the excited state as described by TICT model [33].

The potential energy surface along another possible twisting coordinate (θ_2), i.e., twisting at the acceptor group is shown in Fig. 11 [43]. Grabowski et al. [5] did not support twisting of acceptor group for 'anomalous' charge transfer emission band. But in case of *t*-MMPAA the energy of the S_0 and S_2 states increases and reaches a maximum at $\theta_2 = 90.0^\circ$ in vacuum and in acetonitrile solvent. However, the S_1 state is stabilized at $\theta_2 = 90.0^\circ$. Molecular orbital picture (Fig. 10c) shows that the HOMO at $\theta_2 = 90.0^\circ$ configuration is same as the HOMO of the global optimized structure, but the LUMO is different. In this case the first single excitation is $\pi_{benzene} \rightarrow \pi_{acceptor}$ type of transition. The ground and first excited state molecular orbitals

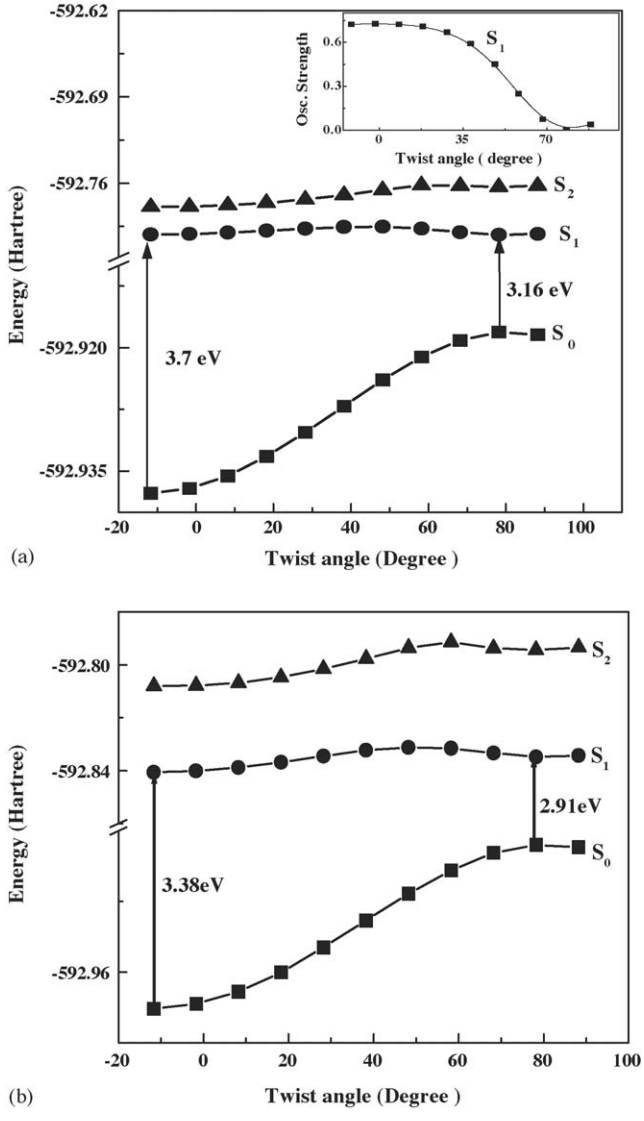

Fig. 9. Potential energy surfaces for the ground and first two excited states along the twisting coordinate at the donor (–NHMe) part in (a) vacuo and (b) acetonitrile solvent using DFT (B3LYP/6-31++g(d,p)) method. *Inset:* plot of the variation of oscillator strength vs. twist coordinate in vacuo.

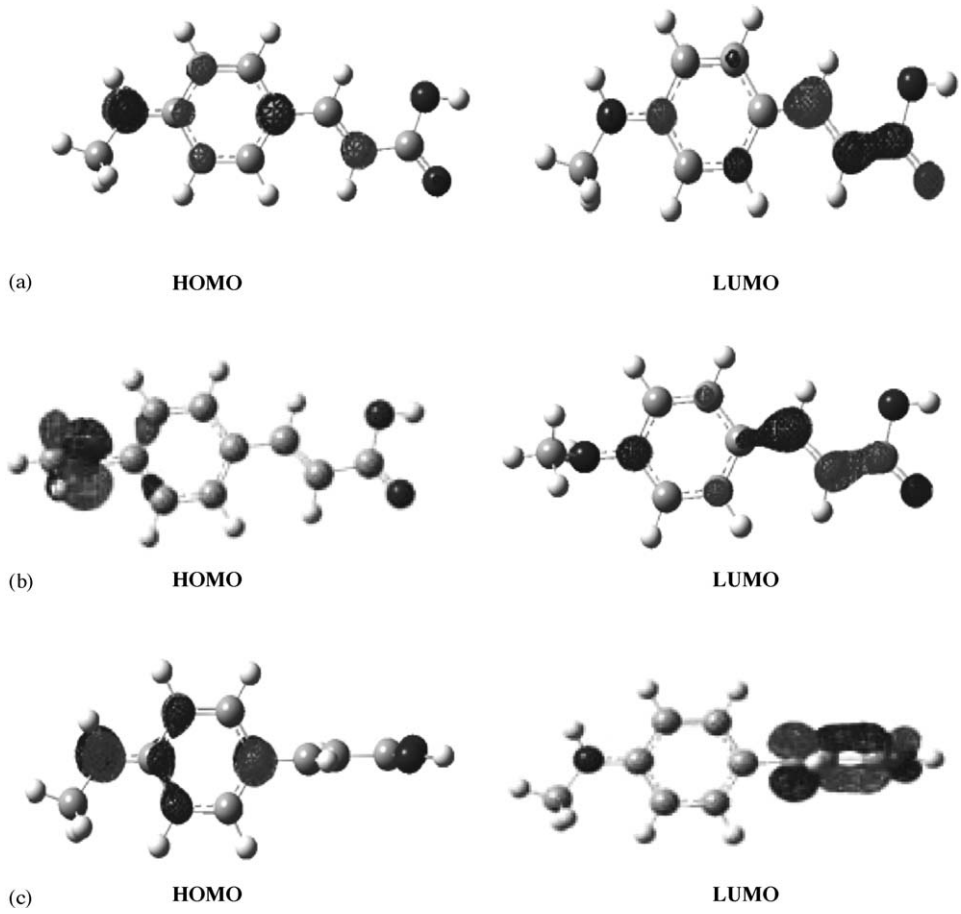

Fig. 10. Molecular orbital for the (a) optimized ground state structure, (b) twisted conformer due to the rotation of monomethylamino group and (c) twisted conformer due to rotation of acceptor (–CH=CHCOOH) group.

(Fig. 11a, inset) are perpendicular to each other and hence, this transition is forbidden with low oscillator strength ($f = 0.0002$). In this twisted configuration the nitrogen lone pair is no more available due to delocalization over the benzene ring.

The calculated emission energies of the twisted conformer for the two possible twisting motions in vacuum and in acetonitrile are shown in Table 4. Experimentally *t*-MMPAA shows emission at ~385 nm (3.22 eV) in non-polar medium and at ~437 nm

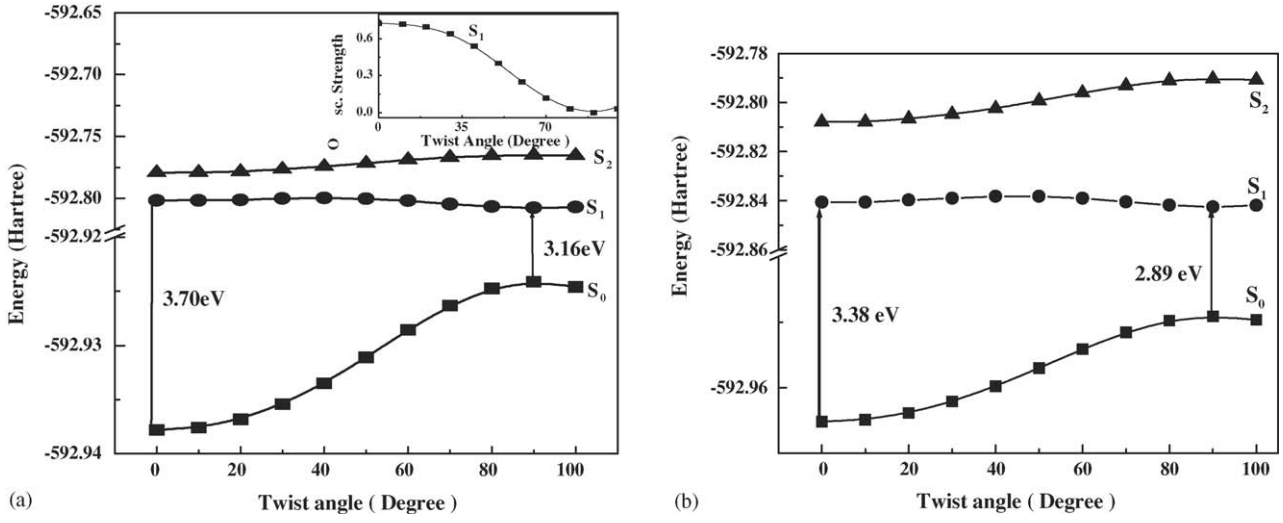

Fig. 11. Potential energy surfaces for the ground and first two excited states along twisting coordinate at the acceptor (–CH=CHCOOH) part in (a) vacuo and (b) acetonitrile solvent using DFT (B3LYP/6-31++g(d,p)) method. *Inset:* plot of the variation of oscillator strength vs. twist coordinate in vacuo.

(2.83 eV) in polar aprotic acetonitrile solvent. For the twisting of the donor part, the calculated emission energies are 3.16 eV (392 nm) and 2.91 eV (425 nm) in vacuo and acetonitrile solvent, respectively. For the twisting of the acceptor part the emission energy in vacuum and in acetonitrile is 3.16 eV (392 nm) and 2.89 eV (427 nm), respectively. So, the transition energies both in vacuum and in acetonitrile along the two twisting paths correlate well with the experimental observation. Large Stokes shift of solvent dependent emission band obtained from theoretical calculation and experimental observation strongly supports the fact that intramolecular charge transfer occurs in the excited state through a twisting process. The little discrepancy between the calculated and measured emission and absorption data may be due to the consideration of non-optimized-excited state geometry in the calculation.

After analyzing the potential energy curves along the two possible twisting coordinates we can conclude that twisting along the acceptor side is energetically favorable over twisting along the donor path. However, molecular orbital pictures predict the feasibility of charge transfer process by twisting of donor group having localized charge at the nitrogen center. Therefore, theoretically we can say that any of the two twisting paths is responsible for excited state relaxation process. But for a definite prediction it needs more effective evidences and rigorous theoretical calculations.

4. Conclusion

In this paper, we have investigated photo-induced charge transfer reaction of a synthesized donor–acceptor substituted aromatic system namely 3-(4-monomethylamino-phenyl)-acrylic acid (*t*-MMPAA) having secondary amine as charge donor, which is still very uncommon. We have studied the photophysical properties of *t*-MMPAA in different polar and non-polar solvents by absorption and emission spectroscopy. The effect of acid, solvent polarity and temperature variation on the spectra, emission properties in 77 K glass matrix and dipole moment of excited state establish well the existence of photoinduced intramolecular charge transfer reaction in *t*-MMPAA molecule. Intermolecular hydrogen bond formation with protic solvents influences the ground and excited states properties of *t*-MMPAA molecule. The microscopic mechanism of intramolecular charge transfer in *t*-MMPAA has been explored theoretically by TDDFT method including solvent effect via PCM model. We have constructed the potential energy surfaces for the ground and different excited states following the twisted intramolecular charge transfer model. It is found that twisting of both the donor and acceptor paths stabilize the S_1 energy state. Calculation shows that twisting along the acceptor group favors energetically over the twisting of donor path. However, the MO structure supports that twisting along the donor path is responsible for CT fluorescence in *t*-MMPAA molecule.

Acknowledgements

This work is supported by a grant from DST, India (Project No. SP/S1/PC-1/2003). N.G. would like to thank Prof. Mihir Chowdhury and Dr. D.N. Nath of IACS, Kolkata for their constant encouragement through out this work. The authors acknowledge Professor Sanjib Ghosh, Department of Chemistry, Presidency College, Kolkata for providing us fluorescence lifetime measurement facility. We thank Mr. Shayam Sundar Maity and Mr. Subhadeep Samanta, Department of Chemistry, Presidency College, Calcutta for helping in lifetime measurement. The authors would like to thank the reviewers for critical comments and suggestions.

References

[1] E. Lippert, W. Luder, Advances in Molecular Spectroscopy, Pergamon Press, Oxford, 1962, p. 443.
[2] W. Rettig, Angew. Chem. Int. Ed. Engl. 25 (1986) 971–988.
[3] W. Rettig, Top. Curr. Chem. 169 (1994) 253–299.
[4] K. Rotkiewicz, K.H. Grellmann, Z.R. Grabowski, Chem. Phys. Lett. 19 (1973) 315–318.
[5] Z.R. Grabowski, J. Dobkowski, W. Kuhnle, J. Mol. Struct. 114 (1984) 93–100.
[6] K.A. Zachariasse, M. Grobys, E. Tauer, Chem. Phys. Lett. 274 (1997) 372–382.
[7] K.A. Zachariasse, T. von der Haar, A. Hebecker, U. Leinhos, W. Kuhnle, Pure Appl. Chem. 65 (1993) 1745–1750.
[8] A.L. Sobolewski, W. Domcke, Chem. Phys. Lett. 259 (1996) 119–127.
[9] D. Rapport, F. Furche, J. Am. Chem. Soc. 126 (2004) 1277–1284.
[10] C.J. Jodicke, H.-P. Luthi, J. Chem. Phys. 117 (2002) 4146–4156.
[11] C.J. Jodicke, H.-P. Luthi, J. Chem. Phys. 119 (2003) 12852–12862.
[12] C.J. Jodicke, H.-P. Luthi, J. Am. Chem. Soc. 125 (2003) 252–264.
[13] A.D. Gorse, M. Pesquer, J. Phys. Chem. 99 (1995) 4039–4049.
[14] P.R. Bangal, S. Chakravorti, J. Photochem. Photobiol. A: Chem. 116 (1998) 191–202.
[15] I. Szydlowska, A. Kyrychenko, J. Nowacki, J. Herbich, Phys. Chem. Chem. Phys. 5 (2003) 1032–1038.
[16] K. Rotkiewicz, W. Rettig, J. Lumin. 54 (1992) 221–229.
[17] C.J. Jodicke, H-P. Luthi, J. Chem. Phys. 117 (2002) 4157–4167.
[18] X.-H. Duan, X.-Y. Li, R.-X. He, X.-M. Cheng, J. Chem. Phys. 122 (2005) 084314-1-084314-9.
[19] R. Cammi, B. Mennucci, J. Tomasi, J. Phys. Chem. A 104 (2000) 5631–5637.
[20] A. Chakraborty, S. Kar, N. Guchhait, in press.
[21] S.K. Pal, S.K. Batabyal, T. Ganguly, Chem. Phys. Lett. 406 (2005) 420–424.
[22] P.R. Bevington, Data Reduction and Error Analysis for the Physical Sciences, Mc GrawHill, New York, 1969.
[23] D. Connor, D. Phillips, Time Correlated Single Photon Counting, Academic Press, London, 1984.
[24] M.J. Frisch, et al., Gaussian 03, Revision B.03, Gaussian Inc., Pittsburgh PA, 2003.
[25] A.B.J. Parusel, Phys. Chem. Chem. Phys. 24 (2000) 5545–5552.
[26] A.B.J. Parusel, W. Rettig, W. Sudholt, J. Phys. Chem. A 106 (2002) 804–815.
[27] A.B.J. Parusel, Chem. Phys. Lett. 340 (2001) 531–537.
[28] L. Serrano-Andres, M. Merchan, B.O. Roos, R. Lindh, J. Am. Chem. Soc. 117 (1995) 3189–3204.
[29] A. Kohn, C. Hattig, J. Am. Chem. Soc. 126 (2004) 7399–7410.
[30] S. Zilberg, Y. Haas, J. Phys. Chem. A 106 (2000) 1–11.
[31] X. Xu, Z. Cao, Q. Zhang, J. Chem. Phys. 122 (2005) 194305–194309.
[32] J. Platt, J. Chem. Phys. 17 (1949) 484–495.
[33] Z. Grabowski, K. Rotkiewicz, W. Rettig, Chem. Rev. 103 (2003) 3899–4032.
[34] C. Cazeau-Dubroca, S. Ait Lyazidi, P. Cambou, A. Peirigua, Ph. Cazeau, M. Pesquer, J. Phys. Chem. 93 (1989) 2347–2358.
[35] N. Mataga, H. Chosrowjan, S. Taniguchi, J. Photochem. Photobiol. C: Photochem. Rev. 6 (2005) 37–79.
[36] F.D. Lewis, W. Weigel, J. Phys. Chem. A 104 (2000) 8146–8153.

[37] R.W. Taft, M.J. Kamlet, J. Am. Chem. Soc. 98 (1976) 2886–2894.
[38] A.C. Testa, J. Lumin. 50 (1991) 243–248.
[39] N. Ghoneim, P. Suppan, Pure Appl. Chem. 65 (1993) 1739–1743.
[40] V. Thiagarajan, C. Selvaraju, E.J. Padma Malar, P. Ramamurty, Chem. Phys. Chem. 5 (2004) 1200–1209.
[41] N. Ikeda, H. Miyasaka, T. Okada, N. Mataga, J. Am. Chem. Soc. 105 (1983) 5206–5211.
[42] J. Herbich, A. Kapturkiewicz, Chem. Phys. 158 (1991) 143–153.
[43] A. Chakraborty, S. Kar, N. Guchhait, Chem. Phys. (2005).